Published in final edited form as:
J Immunol. 2009 October 15; 183(8): 5104–5112. doi:10.4049/jimmunol.0802728.

Phospholipase D Promotes Lipid Microdomain-Associated Signaling Events in Mast Cells[1]

Felipe A. Lisboa[*], **Ze Peng**[*], **Christian A. Combs**[†], and **Michael A. Beaven**[*,2]

[*] Laboratory of Molecular Immunology, National Heart, Lung, and Blood Institute, National Institutes of Health, Bethesda, MD 20892

[†] Light Microscopy Core Facility, National Heart, Lung, and Blood Institute, National Institutes of Health, Bethesda, MD 20892

Abstract

Initial IgE-dependent signaling events are associated with detergent-resistant membrane microdomains. Following Ag stimulation, the IgE-receptor (FcεRI) accumulates within these domains. This facilitates the phosphorylation of FcεRI subunits by the Src kinase, Lyn, and the interaction with adaptor proteins, such as the linker for activation of T cells. Among the phospholipases (PL) subsequently activated, PLD is of interest because of its presence in lipid microdomains and the possibility that its product, phosphatidic acid, may regulate signal transduction and membrane trafficking. We find that in Ag-stimulated RBL-2H3 mast cells, the association of FcεRI with detergent-resistant membrane fractions is inhibited by 1-butanol, which subverts production of phosphatidic acid to the biologically inert phosphatidylbutanol. Furthermore, the knockdown of PLD2, and to a lesser extent PLD1 with small inhibitory RNAs, also suppressed the accumulation of FcεRI and Lyn in these fractions as well as the phosphorylation of Src kinases, FcεRI, linker for activation of T cells, and degranulation. These effects were accompanied by changes in distribution of the lipid microdomain component, ganglioside 1, in the plasma membrane as determined by binding of fluorescent-tagged cholera toxin B subunit and confocal microscopy in live cells. Collectively, these findings suggest that PLD activity plays an important role in promoting IgE-dependent signaling events within lipid microdomains in mast cells.

Stimulation of cells through multimeric immune receptors is accompanied by dynamic reorganization of specialized microdomains of the plasma membrane and this reorganization may play a critical role in signal transduction across the membrane (1,2). These microdomains are enriched in sphingolipids, cholesterol, glycerophospholipids, and glycosylphosphatidylinositol-anchored proteins, and are thought to facilitate such transduction (3). These domains are variously referred as lipid rafts, glycosylphosphatidylinositol-enriched domains, or lipid microdomains although there is considerable debate as to their heterogeneity and function (4–6). Lipid microdomains are thought to participate in the early signaling events following activation of mast cells by Ag via the high affinity receptor for IgE, FcεRI (7,8).

[1]This work was supported by the intramural program of the National Heart, Lung, and Blood Institute at the National Institutes of Health.

[2]Address correspondence and reprint requests to Michael A. Beaven, Room 8N109/Building 10, National Institutes of Health, Bethesda, MD 20892-1760. beavenm@nhlbi.nih.gov.

F.A.L. performed all experiments, created the figures, and prepared a draft of the manuscript in consultation with other authors; Z.P. prepared and evaluated PLD siRNA constructs which were used in the initial studies of this project; C.A.C. advised and assisted in the microscopic studies; and M.A.B. was responsible for the direction and scope of research and for the final version of the manuscript.

Disclosures

The authors have no financial conflict of interest.

Mast cells are stimulated by multivalent binding of Ag to induce clustering of the IgE/FcεRI complex. Ag-induced clustering of FcεRI results in tyrosine phosphorylation of its β and γ subunits by the Src kinase, Lyn (9). This phosphorylation allows recruitment of additional Lyn molecules and the phosphorylation and activation of Syk tyrosine kinase, which is critical for initiation of several downstream phosphorylation signaling pathways (10). One such pathway, the phosphorylation of the linker for activation of T cells (LAT),[3] primarily by Syk, allows recruitment and assembly of additional adaptor and effector molecules facilitating further propagation of signals (11).

Following Ag-induced aggregation, FcεRI localizes in detergent-resistant fractions obtained by gradient centrifugation that are enriched in active Lyn (12), cholesterol, glycosphingolipids, and sphingomyelin (13). The subsequent phosphorylation events appear to occur within these domains (12,14,15). As a further refinement of this model, these domains may regulate Lyn activity due to the exclusion of phosphatases from lipid rafts (16). However, it has been reported that tyrosine phosphorylation of FcεRI can occur outside the confines of detergent-resistant membrane fractions (17) and its dephosphorylation within these fractions (18).

The two isoforms of phospholipase D (PLD), PLD1, and PLD2, and its product, phosphatidic acid (PA), have been implicated in a variety of signaling and membrane trafficking events in different cell types (19,20), including signaling processes (21,22), degranulation (22–25), and actin-dependent membrane ruffling (26) in mast cells. There is evidence that PLD is localized in lipid rafts in RBL-2H3 cells. Studies with overexpressed PLDs suggest that only a small fraction of PLD1 is localized in detergent-resistant membrane fractions in nonstimulated cells (27), but such localization is enhanced in Ag-stimulated cells (28). The activation of PLD by Ag is inhibited by short chain ceramides, thought to act via disruption of lipid microdomains (29). Also, overexpressed fluorescent-tagged PLD2 colocalizes with endogenous LAT (22), which is associated with lipid microdomains in T cells (30) and mast cells (15).

In this study, we have investigated whether PLD plays a role in FcεRI-mediated signaling events that are associated with lipid microdomains. To minimize the possible dissociation of Ag from IgE and FcεRI subunits from each other (18,31), we resorted to a simple stepwise centrifugation separation procedure to isolate a detergent-resistant fraction containing lipid microdomains as described by others (32). Although this fraction probably contains extraneous material, we find that the distribution and phosphorylation of FcεRI and tyrosine kinases follows the same pattern as that described by others for detergent-resistant lipid microdomains in mast cells (12,14,15). As an additional approach, the effects of PLD deficiency on lipid microdomain assembly were evaluated by confocal microscopy using fluorescent-tagged cholera toxin (CTx) B-subunit, which binds ganglioside 1 (GM1), a component of lipid microdomains (33).

Materials and Methods

Materials

Reagents were from the following sources: culture reagents from Life Technologies/Life Technologies; normal butyl alcohol (1-butanol) from Mallinckrodt; Tris from INC Biomedicals; mAb against FcεRI β-subunit was provided by Dr. Juan Rivera (National Institute of Arthritis and Musculoskeletal and Skin Diseases/National Institutes of Health); Abs against FcεRI γ-subunit, LAT, phospho-LAT Tyr226, and phosphotyrosine clone 4G10 from Millipore; Abs against Lyn, phospho-Src Tyr416, LAT, phospho-LAT Tyr171, phospho-LAT Tyr191 from Cell Signaling Technology; Abs against Thy-1, PLD1 and PLD2 from Santa Cruz

[3]Abbreviations used in this paper: LAT, linker for activation of T cells; PL, phospholipase; PA, phosphatidic acid; CTx, cholera toxin; GM1, ganglioside1; MβCD, methyl beta cyclodextrin; PIP2, phosphatidylinositol bisphosphate; siRNA, small inhibitory RNA.

Biotechnology; Ab against mouse FcεRI α-subunit PE conjugated clone MAR-1 and isotype control from eBioscience; Vybrant Alexa Fluor 488 and 594 lipid raft labeling kits and NuPage LDS sample buffer 4× from Invitrogen; PLD1, PLD 2, and GAPDH plasmids from Integrated DNA Technologies; ON-TARGETplus SMARTpool rat PLD1 and PLD2 small inhibitory RNA (siRNA) constructs from Dharmacon; pmaxGFP from Amaxa; and monoclonal anti-DNP IgE Ab (SPE-7), Ag (Ag, DNP-HSA, dinitrophenylated human serum albumin), and all other reagents from Sigma-Aldrich.

Cell culture and experimental conditions

RBL-2H3 cells were grown as monolayers in MEM with Earle's salts, supplemented with glutamine, antibiotics, and 15% FBS. Cells were harvested by trypsinization and transferred to multiwell plates or petri dishes as indicated. Cells were then incubated overnight in complete growth medium that contained DNP-specific IgE (100 ng/ml) to achieve optimal occupancy of FcεRI. Experiments were performed in a PIPES-buffered saline; 25 mM PIPES (pH 7.2), 159 mM NaCl, 5 mM KCl, 0.4 mM MgCl2, 1 mM CaCl2, 5.6 mM glucose, and 0.1% fatty acid-free fraction V from bovine serum. Inhibitors and stimulants were used at concentrations that produced maximal effects.

Isolation of detergent-resistant membrane fractions

Cells were plated overnight in 6-well plates (2×10^6 cells/2 ml/well). Lipid rafts were prepared as described by others (32). In brief, 2×10^6 RBL-2H3 cells were lysed on ice for 20 min in 200 μl of 1% Triton X-100 in 25 mM MES and 150 mM $NaCl_2$ at pH 6.5 (32) and then homogenized with a loose-fitting Dounce homogenizer to obtain the whole cell lysate preparation. The homogenate was centrifuged at 500 × *g* for 7 min at 4°C. The postnuclear supernatant fraction was centrifuged at 100,000 × *g* for 50 min at 4°C to obtain the detergent-soluble membrane fraction. The residual pellet was solubilized in 20 μl of a β-octyl-glucopyranoside buffer to obtain the detergent-resistant fraction. In some experiments, the pellet was dissolved in one third the volume to achieve sufficiently dense immunoblots.

Measurement of AlexaFluor-tagged CTx fluorescence in multiwell plates

Cells were incubated overnight in 96-well black multiwell plates (PerkinElmer) at a density of 2×10^5 cells/0.1 ml/well. The assay was performed as described by others (33), except that cells were labeled with Alexa Fluor 488-tagged CTxB-subunit (300 ng/well for 30 min at 4° C) in the PIPES-buffered medium and washed twice before replenishing the PIPES-buffered medium (0.1 ml). Fluorescence (excitation at 488 nm and emission at >520 nm) was measured by use of a microplate reader (SpectraMax M5, Molecular Devices). The use of microplates allowed direct comparison of the effects of stimulants and inhibitors. A value of $p < 0.05$ was considered as statistically significant.

Flow cytometry

Bone marrow mast cells (3×10^5/group) were incubated with 0.4 μg/ml anti-mouse FcεRI α or isotype control on ice for 30 min in 200 μl of PBS with 0.1% BSA and 0.05% sodium azide followed by washing and treatment using 50 mM 1-butanol or *t*-butanol for 15 min. The cell surface fluorescence intensity was measured using a flow cytometer (FACSCalibur, BD Biosciences). Combined results were analyzed and summarized in a chart using the FlowJo software.

Transfection of siRNA and detection of PLD1 and PLD2 mRNAs by RT-PCR and Western blotting

RBL-2H3 cells were cotransfected with siRNAs against rat PLD1 or PLD2 (2 μM in 5×10^6/0.1 ml) and GFP (pmaxGFP) (1 μg in 5×10^6 cells/0.1 ml) by use of an Amaxa Nucleofector

Device (program T-020). Control cells were transfected with GFP alone. The expression of PLD mRNA in cells was measured at 24 h by real-time PCR (7300 Real Time PCR system, Applied Biosystems) by use of a RNA extraction kit (Qiagen) and the following primers: rat PLD1 sense primer, 5′-GTG GGC AGT GTC AAG CGG GTC ACC-3′, antisense primer, 5′-GCC AAA ACC TAG TCT CCC CAT GGA-3′; rat PLD2 sense primer, 5′-ATG ACT GTA ACC CAG ACG GCA CTC-3′, antisense primer, 5′-CAG CTC CTG AAA GTG TCG GAA TTT-3′; rat GAPDH sense primer, 5′-GTG GAG TCT ACT GGC GTC TTC-3′, antisense primer, 5′-CCA AGG CTG TGG GCA AGG TCA-3′. The expression of PLD1 and PLD2 proteins was determined 48 h after transfection by immunoblotting.

Measurement of degranulation

Cell cultures (5×10^5 cells/0.1 ml/well in 96-well plates) were washed and growth medium was replaced with PIPES-buffered saline medium before stimulation. Degranulation was determined by measurement of release of the granule marker *β*-hexosaminidase by use of a colorimetric assay in which release of *p*-nitrophenol from *p*-nitrophenyl-*N*-acetyl-*β*-D-glucosaminide is measured (34). Values indicate the percent of intracellular *β*-hexosaminidase that was released into the medium.

Live cell imaging using fluorescent optical and confocal laser microscopy

For fluorescent optical microscopy, nontransfected and siRNA-transfected RBL-2H3 cells were incubated with IgE overnight in 24-well plates (2×10^5 cells/0.4 ml/well). Cultures were washed twice, replenished with fresh ice-cold PIPES-buffered saline, and placed on ice. Cells were stained with CTx-Alexa Fluor 488 (400 ng/well for 5 min at 4°C). Cultures were then washed for immediate microscopic examination (Zeiss Axiovert 200 M and a ×20, 0.4 NA objective). Where indicated, 1-butanol (50 mM) or *t*-butanol (50 mM) was added to cultures 15 min before stimulation with Ag. For laser confocal microscopy, transfected cells (25×10^3 cells/ml) were incubated overnight with IgE in 35 mm glass-bottom microwell dishes (MatTek Corporation). For each experiment, cultures were washed with ice-cold PIPES-buffered saline before exposing cells to the specified fluorescent-tagged CTx B-subunit (2 μg/ml/dish) for 2 min at 4°C. Images were acquired with a ×63 (1.4 NA) objective and a confocal laser-scanning microscope (Zeiss LSM510), and analyzed with the pinhole configuration set for a optical slice of 5 μm at 5 μm up from the bottom of the coverslip. pmaxGFP and Alexa Fluor 594 were detected at emission wavelengths of 505–530 nm (excitation at 488 nm), and >610 nm (excitation at 594 nm), respectively. Corrections were made for background fluorescence and fluorescence overlap among fluorophores. Morphometric analysis was performed for the acquired images by measuring changes in a threshold area of the optical slice generated by the signal of fluorescent tagged CTxB (≥ 4 cells/field and ≥ 5 fields/group) before and after treatment with Ag in the same cell. These changes were calculated by dividing the fluorescence within the area encompassed by fluorescent tagged CTxB in the plasma membrane (A) by the sum of this fluorescence and the total fluorescence within the area encompassed by pmaxGFP in the cytosol (B) using the software program Metamorph (Molecular Devices), and comparing the ratio, A/(A+B), obtained before and after treatment. These results were analyzed using a paired *t* test. A value of $p < 0.05$ was considered as statistically significant.

Western blot analysis and immunoprecipitation

Immunoblots were prepared from fractions obtained during the preparation of the detergent-resistant membrane fraction or from whole cell lysates for which cells were lysed in ice-cold lysis buffer: 20 mM HEPES (pH 7.3); 1% Triton X-100; 10% glycerol; 12.5 mM sodium pyrophosphate; 10 mM sodium orthovanadate; 50 mM sodium fluoride; 1 mM PMSF; 30 μg/ml leupeptin; 30 μg/ml aprotinin; and 25 mM *p*-nitrophenyl phosphate. For

immunoprecipitation studies, cells were lysed in the same buffer except that Nonidet P-40 was used instead of Triton-X-100. Immunoprecipitations were then performed as described elsewhere (35). All samples obtained by the above procedures were mixed with one fourth volume of 4× NuPage LDS sample buffer before separation of proteins by use of NuPAGE Novex Bis-Tris gels as described by others (36). Proteins were detected by chemiluminescence (Immobilon Western, Millipore) and quantitated by densitometry (Image Station 2000R, Eastman Kodak). A value of $p < 0.05$ was considered as statistically significant.

Results

Suppression of PA production by 1-butanol impairs association of FcεRIβ with detergent-resistant membrane fractions

The efficacy of the two-step membrane separation procedure was investigated by examination of the distribution of two putative lipid raft markers, Thy1 (1) and LAT (37), as well as FcεRI and Lyn. Both Thy-1 and LAT were confined to the detergent-resistant fraction even after Ag stimulation whereas Lyn and the FcεRIβ subunit were present in both detergent soluble and resistant fractions before stimulation and accumulated in the detergent resistant fraction after Ag addition (Fig. 1*A*, quantitative data are shown in Fig. 1, *B* and *C*). A similar accumulation was observed for the FcεRIγ subunit (data not shown). This apparent redistribution of FcεRI subunits and Lyn was consistent with previous reports in which membrane fractions were separated by sucrose gradients (12,38). Addition of the cholesterol-depleting agent, methyl β-cyclodextrin resulted in substantial loss of FcεRIβ from the detergent resistant fraction in nonstimulated and stimulated cells without affecting the expression of FcεRIβ in whole cells (Fig. 1*C*).

In the absence of low m.w. inhibitors of PLD, 1-butanol has been widely used to divert production of PA by PLD to the biologically inert phosphatidylbutanol through transphosphatidylation (20). The effects of 1-butanol may thus reveal phosphatidate-dependent reactions. Tertiary-butanol is not readily transphosphatidylated and can be used as a control for nonspecific actions of butanol. As shown in Fig. 1*F*, 1-butanol but not tertiary-butanol suppressed the expression of FcεRIβ in the detergent-resistant fraction in nonstimulated and stimulated cells without affecting the total amount of proteins contained in these fraction (Fig. 1*G*) and expression of the receptor in the plasma membrane as observed by flow cytometry (Fig. 1*H*).

1-Butanol also suppresses Ag-induced changes in distribution of fluorescent-tagged CTx B subunit

The redistribution of lipid microdomains in the plasma membrane was also monitored in live cells by use of Alexa Fluor 488-tagged CTxB which forms a stable pentameric structure and binds to the lipid raft component, GM1 (39). Increased fluorescence is thought to indicate redistribution of GM1 in the plasma membrane during lipid raft assembly or additional recruitment of GM1 to the surface membrane (40). Addition of Ag resulted in enhanced surface fluorescence which was substantially diminished in the presence 1-butanol but less so in the presence of tertiary-butanol (Fig. 2*A*). Quantification of the changes in surface fluorescence in a multiwell plate reader also indicated that 1-butanol, but not tertiary-butanol, inhibited the increase in fluorescence (Fig. 2*B*). Additional experiments revealed that direct cross-linking of CTx with an anti-CTx Ab enhanced fluorescence in a time-dependent manner (Fig. 2*C*). However, this increased fluorescence was not affected by either 1-butanol or tertiary-butanol (Fig. 2*D*).

Knockdown of PLD1 and PLD2 by siRNA suppresses association of FcεRI and Lyn with detergent-resistant membrane fractions and redistribution of fluorescent-tagged CTxB

The above studies with butanol suggest that production of PA by PLD is required for optimal assembly and function of lipid microdomains in RBL-2H3 cells. We next investigated the effects of knockdown of PLD1 or PLD2 with siRNAs directed against each of these isoforms. The siRNAs used selectively reduced production of transcripts (Fig. 3*A*) and protein (Fig. 3*B*) of PLD1 and PLD2. Knockdown of either PLD reduced expression of Lyn (Fig. 3*D*) and FcεRI*β* subunit (Fig. 3*E*) in the membrane detergent-resistant fraction from nonstimulated and stimulated cells without affecting the total amount of protein present in these fractions (Fig. 3*C*). However, PLD knockdown had no effect on cellular expression of Lyn or FcεRI*β* (*upper panels*, Fig. 3, *D* and *E*).

Knockdown of the PLDs also altered the distribution of GM1 as indicated by use of the Alexa Fluor 488-tagged CTxB. The enhanced surface fluorescence that is observed after Ag stimulation (i.e., Fig. 2) was suppressed in cells that had been transfected with siRNAs against PLD1 or PLD2 (Fig. 4*A*). The quantitative fluorescence data suggested that knockdown of PLD2 had a more pronounced effect than that of PLD1 (Fig. 4*B*). Knockdown of the PLDs appeared to be as effective as the cholesterol-depleting agent methyl *β*-cyclodextrin in suppressing the increase in fluorescence (Fig. 4*C*). Consistent with previous reports, knockdown of the PLDs (21) and treatment with methyl *β*-cyclodextrin (41) was associated with substantial decrease in Ag-stimulated degranulation (Fig. 4, *D* and *E*).

Effects of knockdown of PLD1 and PLD2 on distribution of GM1 in the plasma membrane as determined by confocal laser microscopy

Exploratory confocal microscopic studies were undertaken to evaluate the use of fluorescent-tagged CTx B-subunit to monitor changes in lipid microdomain distribution. In RBL-2H3 cells colabeled with GFP and Alexa Fluor594 CTx B-subunit, Ag stimulation resulted in recruitment of the CTx B-subunit in larger aggregates at the plasma membrane (Fig. 5*A*). As expected, this recruitment was suppressed in cells treated with methyl *β*-cyclodextrin (Fig. 5*C*). By contrast, there was substantial recruitment of fluorescent labeled CTx at the plasma membrane by direct cross-linking of the CTx B-subunit with anti-B-subunit Ab (Fig. 5*E*). The quantitative data from these experiments are shown in Fig. 5, *B*, *D*, and *F*.

Knockdown of PLD1 with siRNA reduced surface expression of fluorescent-tagged CTx B-subunit as compared with control cells (Fig. 6, *A* and *C*) although, as in control cells, redistribution of the CTx B-subunit was still apparent after Ag stimulation (Fig. 6*C*). Knockdown of PLD2 resulted in a more pronounced reduction of surface binding of CTx B-subunit (Fig. 6*E*) and was visible only at higher exposure than shown in Fig. 6*E*. Morphometric data for all cells are shown in panels *B*, *D*, and *F*.

Effects of knockdown of PLD1 and PLD2 on lipid microdomain-related signaling events

Collectively the previous experiments suggested that diversion of production of PA with 1-butanol or knockdown of the PLDs resulted in dispersal of lipid raft molecules such as GM1 and reduced association of FcεRI and Lyn with lipid microdomains. We next investigated whether such dispersion affects stimulatory events that are associated with lipid microdomains. Disruption of these domains with methyl *β*-cyclodextrin blocked Ag-induced phosphorylation of FcεRI *β*-subunit (Fig. 7*A*) and the linker protein LAT (data not shown). 1-Butanol partially blocked (~50%) the additional phosphorylation of the FcεRI*β*-subunit that was induced by Ag (Fig. 7*B*). As a negative control, *t*-butanol had no effect on this phosphorylation when compared with stimulated control cells. Similarly, knockdown of PLD2 and to a lesser extent PLD1 impaired phosphorylation of FcεRI*β* and LAT in addition to Lyn/Src kinase (Fig. 7, *C*–*E*). LAT contains several tyrosines which when phosphorylated act as key docking sites for various

molecules that allow further propagation of signaling (11). The tyrosine phosphorylation of LAT at three such sites namely, 171, 191, and 226, were reduced (Fig. 7*E*) in PLD-deficient cells consistent with the decrease in total phosphorylation of LAT (as in Fig. 7*E*). However, the reduction in phosphorylation of LAT 226 and total phosphorylation of LAT was most pronounced in PLD2-deficient cells. These results suggest that deficiency in PLD2 and to a lesser extent PLD1 impairs lipid microdomain assembly and associated signaling events.

Discussion

Specialized cholesterol-enriched domains in the plasma membrane are thought to facilitate interaction of molecules that convey signals from membrane receptors to the cell interior (2, 7). However, the nature and heterogeneity of these domains are still a matter of debate (4,6). In contrast to the known lipid components of these microdomains, PLD products have received surprisingly little attention given their reported roles in membrane trafficking and the likely presence of PLD in specialized plasma membrane domains (22,27–29). The present work provides evidence that PLD may participate in lipid microdomain assembly and function, thus promoting mast cell activation.

PLD is thought to regulate signal transduction, cytoskeletal rearrangement, and vesicular trafficking (20), which may represent complementary mechanisms for cell activation. In mast cells specifically, PLD has been implicated in signal transduction, membrane ruffling, endocytosis, and exocytosis (11). PLD-derived PA has been implicated in the activation of protein kinase C (21), phosphatidylinositol 4-phosphate 5-kinase (PIP5-kinase) (26,42), and the mammalian target of rapamycin (43) in mast cells and other types of cells. Overexpressed isoforms of PLD, PLD1, and PLD2, are localized on granules and plasma membrane, respectively, in the RBL-2H3 mast cell line (23,25,28,44). Stimulation of these cells results in fusion of granules, and the association of PLD1, with the plasma membrane. In this location, overexpressed PLD1 colocalizes with actin-rich detergent-resistant structures (28) and is thought to form aggregates with actin along the inner surface of the plasma membrane (45). PLD2-derived PA is reported to regulate Ag-stimulated actin-dependent membrane ruffling by enhancing production of the PIP5-kinase product, phosphatidylyinositol 4,5-bisphosphate (PIP2) (26). These findings suggest a functional role for PLD within plasma membrane domains that are associated with PIP5-kinase and actin.

The present results indicate that diversion of production of PA to phosphatidylbutanol with 1-butanol and knockdown of either PLD1 or PLD2 with siRNAs results in reduced association of FcεRIβ with the detergent-resistant membrane fraction and the enhanced association of FcεRIβ with this fraction following Ag stimulation (Figs. 1 and 3). Similar results were obtained with Lyn after knockdown of the PLDs (Fig. 3). These results resembled those obtained by use of methyl β-cyclodextrin (Fig. 1). Visualization of the distribution of the lipid raft component, GM1, with fluorescent-tagged CTxB also indicated that Ag-induced redistribution of GM1 was suppressed by 1-butanol, knockdown of the PLDs, and methyl β-cyclodextrin (Figs. 2, 4, and 5). However, redistribution of GM1 caused by direct Ab cross-linking of CTxB (Figs. 2*C* and 5*E*) was unaffected by 1-butanol (Fig. 5*D*). High resolution optical microscopy also revealed that the expression of CTx B subunit bound at the plasma membrane was suppressed by knockdown of PLD2 and to a lesser extent PLD1 (Fig. 6).

Knockdown of the PLDs also suppressed signaling events that are thought to be associated with lipid microdomains. These events included the tyrosine phosphorylation of FcεRIβ, Src kinases, and LAT (Fig. 7). Knockdown of PLD2 had the most profound effect on phosphorylation of Src kinases and LAT as might be expected from its location in the plasma membrane although it should be noted that PLD1 appears in the plasma membrane within 5 min after stimulation with Ag (23,28). Depletion of membrane cholesterol with methyl β-

cyclodextrin similarly inhibited phosphorylation of FcεRI*β* (Fig. 6*A*) and its association with detergent-resistant membrane fractions (Fig. 1*C*). Collectively, these data indicate similarity in the effects of methyl *β*-cyclodextrin, and knockdown of the PLD isoforms and suggest that PLD is required for the functional integrity of lipid microdomains. These effects can be attributed to the production of PA by PLD because of the similar actions of 1-butanol and knockdown of PLD.

The role of lipid microdomains or lipid rafts in signal transduction in mast cells is a matter of ongoing investigation and studies provide different perspectives depending on the approaches used (7,8). The presence of glycososphingolipids and cholesterol in an ordered lipid phase is thought to allow concentration of some signaling molecules and the exclusion of others such as phosphatases. For example, LAT (30) and other lipid modified proteins such as Lyn are concentrated in detergent-resistant membrane fractions. In one model, FcεRI is thought to be normally excluded from lipid microdomains, but on aggregation with Ag, FcεRI interacts with these domains to bring it in close proximity to Lyn, which can then phosphorylate the FcεRI subunits, the initial step in the signaling process (12,46). This process leads to the recruitment and phosphorylation of Syk kinase, LAT, and PLC*γ*1, generation of a calcium signal, and degranulation (12). The presence of LAT in detergent-resistant membrane domains facilitates its phosphorylation by tyrosine kinases (30) and the subsequent docking and assembly of signaling molecules such as PLC*γ* (11).

The modern tools of microcrosopy and analytical techniques have allowed more direct examination of the structural dynamics of membrane microdomains in mast cells. Such studies have shown that Ag-stimulated FcεRI form patches within the plasma membrane thought to contain many of the essential signaling components for FcεRI-mediated signaling (8,47,48). These FcεRI patches appear to represent discrete signaling domains that form in a dynamic fashion during the signaling process (49). For example, components of detergent-resistant membrane fraction including Thy1, GM1, and LAT are not normally colocalized with each other or with FcεRI in nonstimulated mast cells but upon stimulation with Ag FcεRI and GM1 accumulate in distinctive patches (49), which are enriched in sphingomyelin and cholesterol (50). However, it is apparent from electron microscopic studies that biochemical detergent-resistant fractions consist of a mixture of domains (48,49). FcεRI and LAT, for example, exist in distinct domains with only transient interaction between them during stimulation. It is also apparent that the interaction of FcεRI with Lyn and other anchored proteins is dependent on F-actin polymerization (51). In general, these studies indicate discrete membrane microdomains, which interact with each other during cell activation.

In this study, we have used both biochemical and live-cell microscopic techniques because of caveats to individual approaches (8). Detergent-resistant fractions may contain an amalgam of domains that exist as distinct entities in native membranes. Conflicting data has emerged from studies with methyl *β*-cyclodextrin and it is apparent the effects of this agent are complex (38,41,52). Indeed, cholesterol depletion may impair certain molecular interactions by altering the biophysical properties of the plasma membrane in addition to disrupting detergent-resistant membrane fractions (1). Studies of cholesterol-deficient mast cells derived from mice that carried a null mutation of the 3 *β*-hydroxysterol-Δ^7-reductase gene suggest that some but not all initial signaling events in mast cells are cholesterol dependent (53).

The present results support the view that both PLD isoforms regulate the assembly of membrane detergent-resistant microdomains that are critical for cell activation. Previous reports of the association of at least one PLD isoform with actin-rich detergent-resistant fractions (28) and F-actin aggregates in the cell periphery (45) in stimulated mast cells raise the possibility that PLD, in partnership with PIP5-kinase, may regulate microdomain structure via cytoskeletal remodeling. Production of PIP2 by PIP5-kinase is dependent on PLD-derived

PA in intact cells (26,54). Actin filaments and microtubules are thought to be the primary cytoskeleton components that interact with lipid rafts (2). Of note, the anchoring and assembly of both actin and tubulin with the plasma membrane is dependent on PIP2 which is known to accumulate in lipid microdomains (2). In addition to activating PIP5-kinase, PA itself can serve as a lipid anchor for recruitment and activation of proteins (55) and alter membrane properties because of its ionic charge and fusogenic properties (20). Therefore, there are multiple mechanisms, possibly complementary, by which activation of PLD could impact the dynamics of signaling events within the vicinity of lipid microdomains.

Acknowledgments

We thank Dr. Yasuko Furumoto (National Institutes of Arthritis and Musculoskelatal and Skin Diseases), Shahin Hassanzadeh, Dr. Daniela Malide (both of the National Heart, Lung, and Blood Institute), and Dr. Cristina Grodzki (National Institute of Dental and Craniofacial Research) for advice on various technical aspects of this study.

References

1. Draber P, Draberova L. Lipid rafts in mast cell signaling. Mol Immunol 2002;38:1247–1252. [PubMed: 12217391]
2. Allen JA, Halverson-Tamboli RA, Rasenick MM. Lipid raft microdomains and neurotransmitter signalling. Nat Rev Neurosci 2007;8:128–140. [PubMed: 17195035]
3. Brown DA, London E. Structure and function of sphingolipid- and cholesterol-rich membrane rafts. J Biol Chem 2000;275:17221–17224. [PubMed: 10770957]
4. Mishra S, Joshi PG. Lipid raft heterogeneity: an enigma. J Neurochem 2007;103(Suppl 1):135–142. [PubMed: 17986148]
5. Shaw AS. Lipid rafts: now you see them, now you don't. Nat Immunol 2006;7:1139–1142. [PubMed: 17053798]
6. Pike LJ. Rafts defined: a report on the Keystone Symposium on Lipid Rafts and Cell Function. J Lipid Res 2006;47:1597–1598. [PubMed: 16645198]
7. Sengupta P, Baird B, Holowka D. Lipid rafts, fluid/fluid phase separation, and their relevance to plasma membrane structure and function. Semin Cell Dev Biol 2007;18:583–590. [PubMed: 17764993]
8. Oliver JM, Pfeiffer JR, Surviladze Z, Steinberg SL, Leiderman K, Sanders ML, Wofsy C, Zhang J, Fan H, Andrews N, et al. Membrane receptor mapping: the membrane topography of Fc εRI signaling. Subcell Biochem 2004;37:3–34. [PubMed: 15376617]
9. Vonakis BM, Haleem-Smith H, Benjamin P, Metzger H. Interaction between the unphosphorylated receptor with high affinity for IgE and Lyn kinase. J Biol Chem 2001;276:1041–1050. [PubMed: 11010962]
10. Siraganian RP. Mast cell signal transduction from the high-affinity IgE receptor. Curr Opin Immunol 2003;15:639–646. [PubMed: 14630197]
11. Rivera J, Gilfillan AM. Molecular regulation of mast cell activation. J Allergy Clin Immunol 2006;117:1214–1225. [PubMed: 16750977]
12. Field KA, Holowka D, Baird B. Compartmentalized activation of the high affinity immunoglobulin E receptor within membrane domains. J Biol Chem 1997;272:4276–4280. [PubMed: 9020144]
13. Fridriksson EK, Shipkova PA, Sheets ED, Holowka D, Baird B, McLafferty FW. Quantitative analysis of phospholipids in functionally important membrane domains from RBL-2H3 mast cells using tandem high-resolution mass spectrometry. Biochemistry 1999;38:8056–8063. [PubMed: 10387050]
14. Holowka D, Sheets ED, Baird B. Interactions between FcεRI and lipid raft components are regulated by the actin cytoskeleton. J Cell Sci 2000;113:1009–1019. [PubMed: 10683149]
15. Sada K, Zhang J, Siraganian RP. SH2 domain-mediated targeting, but not localization, of Syk in the plasma membrane is critical for FcεRI signaling. Blood 2001;97:1352–1359. [PubMed: 11222380]
16. Young RM, Zheng X, Holowka D, Baird B. Reconstitution of regulated phosphorylation of FcεRI by a lipid raft-excluded protein-tyrosine phosphatase. J Biol Chem 2005;280:1230–1235. [PubMed: 15537644]

17. Kovarova M, Tolar P, Arudchandran R, Draberova L, Rivera J, Draber P. Structure-function analysis of Lyn kinase association with lipid rafts and initiation of early signaling events after Fce receptor I aggregation. Mol Cell Biol 2001;21:8318–8328. [PubMed: 11713268]
18. Peirce M, Metzger H. Detergent-resistant microdomains offer no refuge for proteins phosphorylated by the IgE receptor. J Biol Chem 2000;275:34976–34982. [PubMed: 10956655]
19. McDermott M, Wakelam MJ, Morris AJ. Phospholipase D. Biochem Cell Biol 2004;82:225–253. [PubMed: 15052340]
20. Jenkins GM, Frohman MA. Phospholipase D: a lipid centric review. Cell Mol Life Sci 2005;62:2305–2316. [PubMed: 16143829]
21. Peng Z, Beaven MA. An essential role for phospholipase D in the activation of protein kinase C and degranulation in mast cells. J Immunol 2005;174:5201–5208. [PubMed: 15843515]
22. Lee JH, Kim YM, Kim NW, Kim JW, Her E, Kim BK, Kim JH, Ryu SH, Park JW, Seo DW, et al. Phospholipase D2 acts as an essential adaptor protein in the activation of Syk in antigen-stimulated mast cells. Blood 2006;108:956–964. [PubMed: 16861349]
23. Choi WS, Kim YM, Combs C, Frohman MA, Beaven MA. Phospholipase D1 and 2 regulate different phases of exocytosis in mast cells. J Immunol 2002;168:5682–5689. [PubMed: 12023367]
24. Way G, O'Luanaigh N, Cockcroft S. Activation of exocytosis by cross-linking of the IgE receptor is dependent on ADP-ribosylation factor 1-regulated phospholipase D in RBL-2H3 mast cells: evidence that the mechanism of activation is via regulation of phosphatidylinositol 4,5-bisphosphate synthesis. Biochem J 2000;346:63–70. [PubMed: 10657240]
25. Brown FD, Thompson N, Saqid KM, Clark JM, Powner D, Thompson NT, Solari R, Wakelam MJO. Phospholipase D1 localises to secretory granules and lysosomes and is plasmamembrane translocated on cellular stimulation. Curr Biol 1998;8:835–838. [PubMed: 9663393]
26. O'Luanaigh N, Pardo R, Fensome A, Allen-Baume V, Jones D, Holt MR, Cockcroft S. Continual production of phosphatidic acid by phospholipase D is essential for antigen-stimulated membrane ruffling in cultured mast cells. Mol Biol Cell 2002;13:3730–3746. [PubMed: 12388770]
27. Hitomi T, Zhang J, Nicoletti LM, Grodzki AC, Jamur MC, Oliver C, Siraganian RP. Phospholipase D1 regulates high-affinity IgE receptor-induced mast cell degranulation. Blood 2004;104:4122–4128. [PubMed: 15339843]
28. Powner DJ, Hodgkin MN, Wakelam MJ. Antigen-stimulated activation of phospholipase D1b by Rac1, ARF6, and PKCa in RBL-2H3 cells. Mol Biol Cell 2002;13:1252–1262. [PubMed: 11950936]
29. Gidwani A, Brown HA, Holowka D, Baird B. Disruption of lipid order by short-chain ceramides correlates with inhibition of phospholipase D and downstream signaling by FcεRI. J Cell Sci 2003;116:3177–3187. [PubMed: 12829737]
30. Zhang W, Trible RP, Samelson LE. LAT palmitoylation: its essential role in membrane microdomain targeting and tyrosine phosphorylation during T cell activation. Immunity 1998;9:239–246. [PubMed: 9729044]
31. Pierini L, Harris NT, Holowka D, Baird B. Evidence supporting a role for microfilaments in regulating the coupling between poorly dissociable IgE-FcεRI aggregates downstream signaling pathways. Biochemistry 1997;36:7447–7456. [PubMed: 9200693]
32. Gaide O, Favier B, Legler DF, Bonnet D, Brissoni B, Valitutti S, Bron C, Tschopp J, Thome M. CARMA1 is a critical lipid raft-associated regulator of TCR-induced NF-κB activation. Nat Immunol 2002;3:836–843. [PubMed: 12154360]
33. Naal RM, Holowka EP, Baird B, Holowka D. Antigen-stimulated trafficking from the recycling compartment to the plasma membrane in RBL mast cells. Traffic 2003;4:190–200. [PubMed: 12656991]
34. Ozawa K, Szallasi Z, Kazanietz MG, Blumberg PM, Mischak H, Mushinski JF, Beaven MA. Ca^{2+}-Dependent and Ca^{2+}-independent isozymes of protein kinase C mediate exocytosis in antigen-stimulated rat basophilic RBL-2H3 cells: reconstitution of secretory responses with Ca^{2+} and purified isozymes in washed permeabilized cells. J Biol Chem 1993;268:1749–1756. [PubMed: 8420951]
35. Andrade MV, Hiragun T, Beaven MA. Dexamethasone suppresses antigen-induced activation of phosphatidylinositol 3-kinase and downstream responses in mast cells. J Immunol 2004;172:7254–7262. [PubMed: 15187100]

36. Nakamura R, Okunuki H, Ishida S, Saito Y, Teshima R, Sawada J. Gene expression profiling of dexamethasone-treated RBL-2H3 cells: induction of anti-inflammatory molecules. Immunol Lett 2005;98:272–279. [PubMed: 15860228]
37. Janes PW, Ley SC, Magee AI, Kabouridis PS. The role of lipid rafts in T cell antigen receptor (TCR) signaling. Semin Immunol 2000;12:23–34. [PubMed: 10723795]
38. Sheets ED, Holowka D, Baird B. Critical role for cholesterol in Lyn-mediated tyrosine phosphorylation of FcεRI and their association with detergent-resistant membranes. J Cell Biol 1999;145:877–887. [PubMed: 10330413]
39. Lencer WI. Microbes and microbial toxins: paradigms for microbial-mucosal toxins, V: cholera: invasion of the intestinal epithelial barrier by a stably folded protein toxin. Am J Physiol 2001;280:G781–G786.
40. Knight ZA, Feldman ME, Balla A, Balla T, Shokat KM. A membrane capture assay for lipid kinase activity. Nat Protoc 2007;2:2459–2466. [PubMed: 17947987]
41. Yamashita T, Yamaguchi T, Murakami K, Nagasawa S. Detergent-resistant membrane domains are required for mast cell activation but dispensable for tyrosine phosphorylation upon aggregation of the high affinity receptor for IgE. J Biochem 2001;129:861–868. [PubMed: 11388899]
42. Jenkins GH, Fisette PL, Anderson RA. Type I phosphatidylinositol 4-phosphate 5-kinase isoforms are specifically stimulated by phosphatidic acid. J Biol Chem 1994;269:11547–11554. [PubMed: 8157686]
43. Foster DA. Phosphatidic acid signaling to mTOR: signals for the survival of human cancer cells. Biochim Biophys Acta 2009;1791:949–955. [PubMed: 19264150]
44. Sarri E, Pardo R, Fensome-Green A, Cockcroft S. Endogenous phospholipase D2 localises to the plasma membrane of RBL-2H3 mast cells and can be distinguished from ARF-stimulated phospholipase D1 activity by its specific sensitivity to Oleic acid. Biochem J 2002;369:319–329. [PubMed: 12374567]
45. Farquhar MJ, Powner DJ, Levine BA, Wright MH, Ladds G, Hodgkin MN. Interaction of PLD1b with actin in antigen-stimulated mast cells. Cell Signal 2007;19:349–358. [PubMed: 16978840]
46. Holowka D, Gosse JA, Hammond AT, Han X, Sengupta P, Smith NL, Wagenknecht-Wiesner A, Wu M, Young RM, Baird B. Lipid segregation and IgE receptor signaling: a decade of progress. Biochim Biophys Acta 2005;1746:252–259. [PubMed: 16054713]
47. Wilson BS, Pfeiffer JR, Oliver JM. Observing FcεRI signaling from the inside of the mast cell membrane. J Cell Biol 2000;149:1131–1142. [PubMed: 10831616]
48. Wilson BS, Pfeiffer JR, Surviladze Z, Gaudet EA, Oliver JM. High resolution mapping of mast cell membranes reveals primary and secondary domains of FcεRI and LAT. J Cell Biol 2001;154:645–658. [PubMed: 11489921]
49. Wilson BS, Steinberg SL, Liederman K, Pfeiffer JR, Surviladze Z, Zhang J, Samelson LE, Yang LH, Kotula PG, Oliver JM. Markers for detergent-resistant lipid rafts occupy distinct and dynamic domains in native membranes. Mol Biol Cell 2004;15:2580–2592. [PubMed: 15034144]
50. Surviladze Z, Harrison KA, Murphy RC, Wilson BS. FcεRI and Thy-1 domains have unique protein and lipid compositions. J Lipid Res 2007;48:1325–1335. [PubMed: 17387221]
51. Wu M, Holowka D, Craighead HG, Baird B. Visualization of plasma membrane compartmentalization with patterned lipid bilayers. Proc Natl Acad Sci USA 2004;101:13798–13803. [PubMed: 15356342]
52. Surviladze Z, Draberova L, Kovarova M, Boubelik M, Draber P. Differential sensitivity to acute cholesterol lowering of activation mediated via the high-affinity IgE receptor and Thy-1 glycoprotein. Eur J Immunol 2001;31:1–10. [PubMed: 11169432]
53. Kovarova M, Wassif CA, Odom S, Liao K, Porter FD, Rivera J. Cholesterol deficiency in a mouse model of Smith-Lemli-Opitz syndrome reveals increased mast cell responsiveness. J Exp Med 2006;203:1161–1171. [PubMed: 16618793]
54. Jarquin-Pardo M, Fitzpatrick A, Galiano FJ, First EA, Davis JN. Phosphatidic acid regulates the affinity of the murine phosphatidylinositol 4-phosphate 5-kinase-Ib for phosphatidylinositol-4-phosphate. J Cell Biochem 2007;100:112–128. [PubMed: 16888807]
55. Chae YC, Kim JH, Kim KL, Kim HW, Lee HY, Heo WD, Meyer T, Suh PG, Ryu SH. Phospholipase D activity regulates integrin-mediated cell spreading and migration by inducing GTP-Rac translocation to the plasma membrane. Mol Biol Cell 2008;19:3111–3123. [PubMed: 18480413]

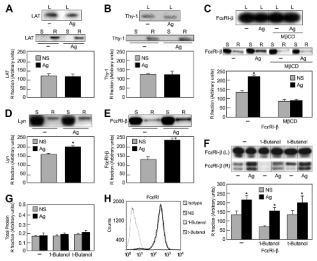

FIGURE 1.

Ag-induced accumulation of FcεRI*β* in the detergent resistant fraction is suppressed by methyl *β*-cyclodextrin and 1-butanol. (*A*, *B*, *D*, and *E*) RBL-2H3 cells were stimulated with Ag (Ag, 100 ng/ml DNP-BSA) for 5 min before fractionation of soluble (S) and detergent-resistant (R) membrane fractions by the two-step fractionation procedure. Immunoblots were prepared for detection of lipid microdomain components, LAT and Thy-1, as well as Lyn and FcεRI*β*. Densitometric data from three such experiments are shown for the amount of LAT, Thy-1, Lyn, and FcεRI*β* in the detergent-resistant fraction. *C*, Cells were treated with the cholesterol-depleting agent methyl *β*-cyclodextrin (M*β*CD) (25 *μ*M) for 30 min or left untreated before stimulation with Ag. The immunoblots show distribution of FcεRI*β* in the soluble (S) and detergent-resistant (R) fractions and the bar graph indicate densitometric data for FcεRI*β* in fraction R from three experiments. *F*, Cells were exposed to 50 mM 1-butanol or *t*-butanol for 15 min before stimulation with Ag for 5 min. The immunoblots indicate the presence of FcεRI*β* in whole cell lysates (L) and the detergent-resistant membrane fraction (R). Densitometric data from three experiments are shown to indicate the levels of FcεRI*β* in the R fraction. Values indicate mean ± SEM and asterisks significant increases at $p < 0.05$. Total amount of protein present in R fraction (*G*) and distribution of FcεRI*β* in plasma membrane of control, 1-butanol-, and *t*-butanol-treated cells as determined by flow cytometry (*H*) are also shown.

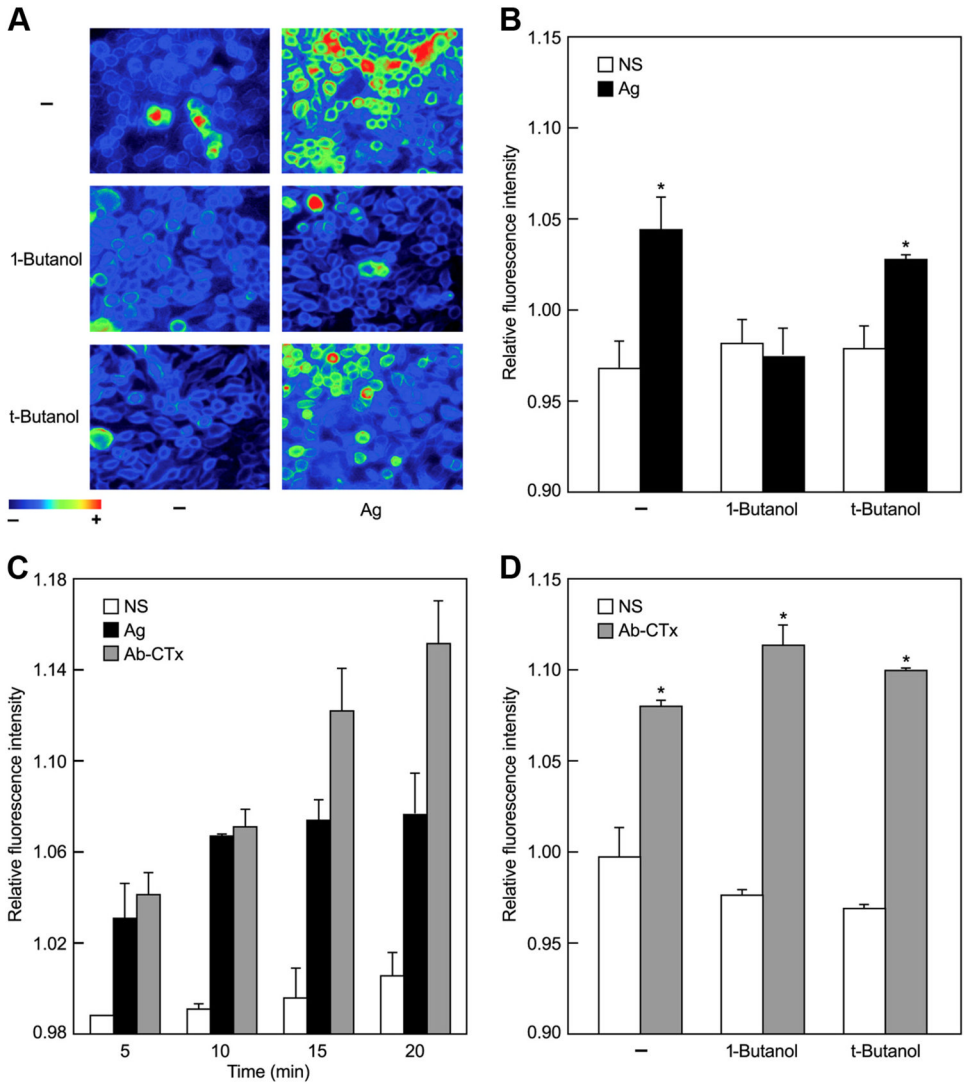

FIGURE 2.

1-Butanol suppresses Ag-induced changes in GM1 surface expression as monitored by fluorescent-tagged CTx B-subunit (CTxB). RBL-2H3 cells were exposed to 1-butanol, tertiary-butanol or neither for 15 min before addition of the Alexa Fluor 488-tagged CTx B-subunit which binds to GM1, present in lipid microdomain. Cells were stimulated, or not (NS), with Ag (Ag, 1 μg/ml DNP-BSA) for 5 min (*A*), 20 min (*B* and *D*), or as indicated (*C*). *A*, Changes in fluorescence intensity were monitored by optical microscopy and shown here after pseudocolor reconstruction. *B–D*, Changes in fluorescence intensity of cell cultures were measured directly in a microplate reader to assess the effects of the butanols in Ag stimulated cells (*B*), the time-course of response to Ag or direct cross-linking of CTx B-subunit with specific Ab (*C*), and the effects of the butanols on changes in fluorescence induced by anti-CTxB Ab (*D*). The data in panels *B–D* are the mean ± SEM of values from three cultures and are representative of two additional experiments. All values depict fluorescence intensity as a ratio of that at the time of addition of Ag or anti-CTxB Ab.

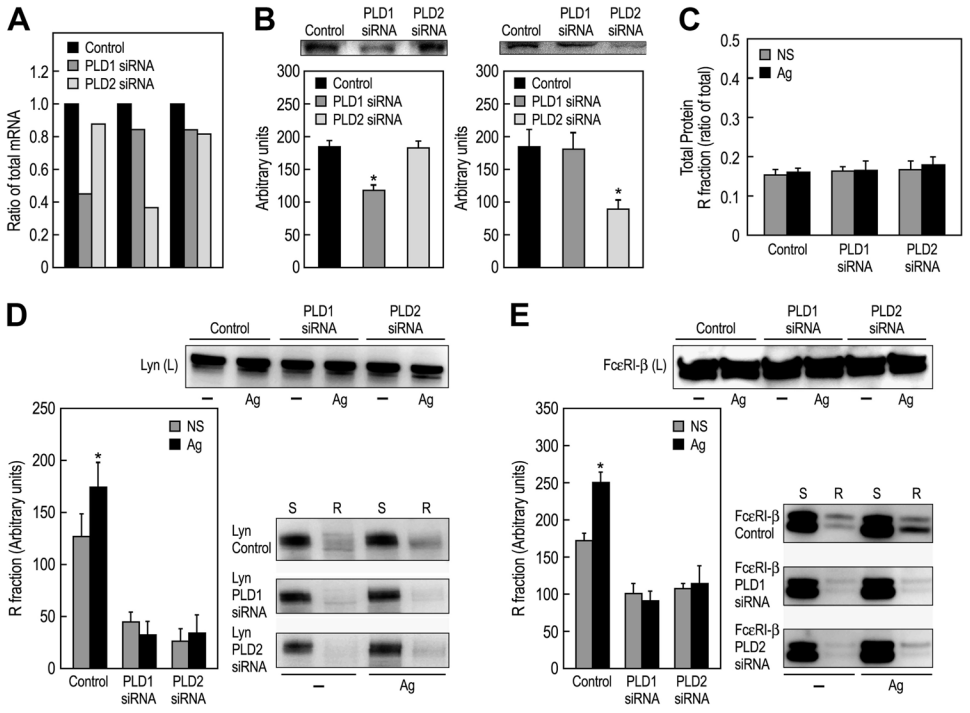

FIGURE 3.

Knockdown of PLD impairs association of Lyn and FcεRI*β* with the detergent-resistant membrane fraction. RBL-2H3 cells were transfected with siRNAs against PLD1 or PLD2 and the indicated levels of transcripts (*A*) and protein (*B*) were measured 24 (*A*) and 48 h (*B*) later. Typical PLD immunoblots are shown in the insets in *B. C*, Total amount of protein present in R fraction of control and PLD siRNA-treated cells. *D* and *E*, Typical immunoblots and densitometric data are shown for the distribution of Lyn and FcεRI*β* in soluble (S) and detergent-resistant (R) membrane fractions in nonstimulated and Ag- stimulated (Ag, 100 ng/ml DNP-BSA) cells. Expression of these two proteins in whole cell lysates (L) is also shown.

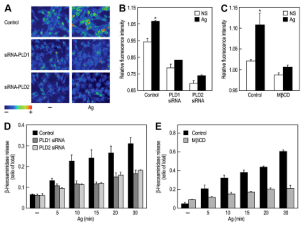

FIGURE 4.

Knockdown of PLD suppresses Ag-induced changes in surface expression of GM1 and degranulation. Experiments were performed with Alexa Fluor 488-tagged CTxB as described for Fig. 2 in control RBL-2H3 cells and cells that had been transfected for 48 h with siRNAs against PLD1 and PLD2. Changes in fluorescence were monitored by microscopy (*A*) and in a microplate reader (*B* and *C*) in non-stimulated (NS) and Ag (Ag, 1 μg/ml, DNP-BSA)-stimulated cells. In *C*, cultures were exposed to methyl β-cyclodextrin (MβCD) (25 mM) for 30 min before stimulation with Ag for comparison with the effects of PLD knockdown in *B*. *D* and *E*, The effects of knockdown of the PLDs and methyl β-cyclodextrin on the time-course of release of the granule marker, β-hexosaminidase are shown. Data are mean ± SEM of values from three cultures and are representative of at least two experiments. Asterisks indicate significant increase at the $p < 0.05$ level.

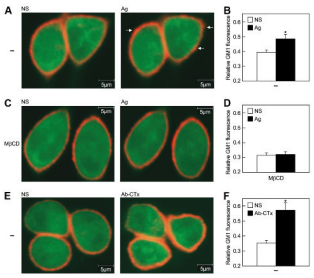

FIGURE 5.

Effect of methyl *β*-cyclodextrin on Ag-induced redistribution of fluorescent-tagged CTxB as determined by confocal laser microscopy. Cells transfected with GFP (pmaxGFP) were labeled with Alexa Fluor 594-tagged CTxB. *A*, *C*, and *E*, Changes in distribution of the CTx B-subunit are shown in the same cells before and after stimulation with Ag in nontreated cells (*A*) and in cells treated with methyl *β*-cyclodextrin (*C*) as well as after direct engagement of CTxB with anti-CTxB Ab (*E*). Experimental conditions were as described for Fig. 2. The micrographs show a segment 5 *μ*m thick, 5 *μ*m from the base of each cell. *B*, *D*, and *F*. Representative quantitative morphometric data are shown for CTxB fluorescence. Values are calculated as a ratio of Alexa Fluor CTxB fluorescence over total fluorescence of CTxB and GFP as described in *Materials and Methods*.

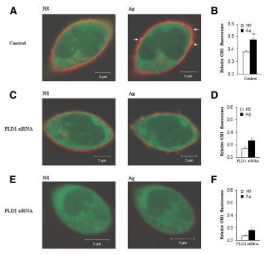

FIGURE 6.

Effect of knockdown of PLD on surface distribution of GM1 as determined by use of fluorescent-tagged CTxB and confocal laser microscopy. Cells were cotransfected with siRNAs against the PLDs and GFP (pmaxGFP) to allow selection of transfected cells. Cells were then labeled with Alexa Fluor 594-tagged CTxB and were stimulated with Ag for 5 min. Transfected cells were selected and monitored by confocal microscopy for both fluorophores. *A*, *C*, and *E*, Fluorescence indicative of CTxB (red) and green fluorescence protein (green), the arrows indicate examples of increased accumulation of CTxB following Ag stimulation (Ag, 1 μg/ml DNP-BSA). *B*, *D*, and *F* show morphometric data for the effects of knockdown of PLD1 and PLD2 on the fluorescence intensity associated with CTxB binding in the plasma membrane. Values are calculated as a ratio of Alexa Fluor CTxB fluorescence over total fluorescence of CTxB and GFP as described in *Materials and Methods*.

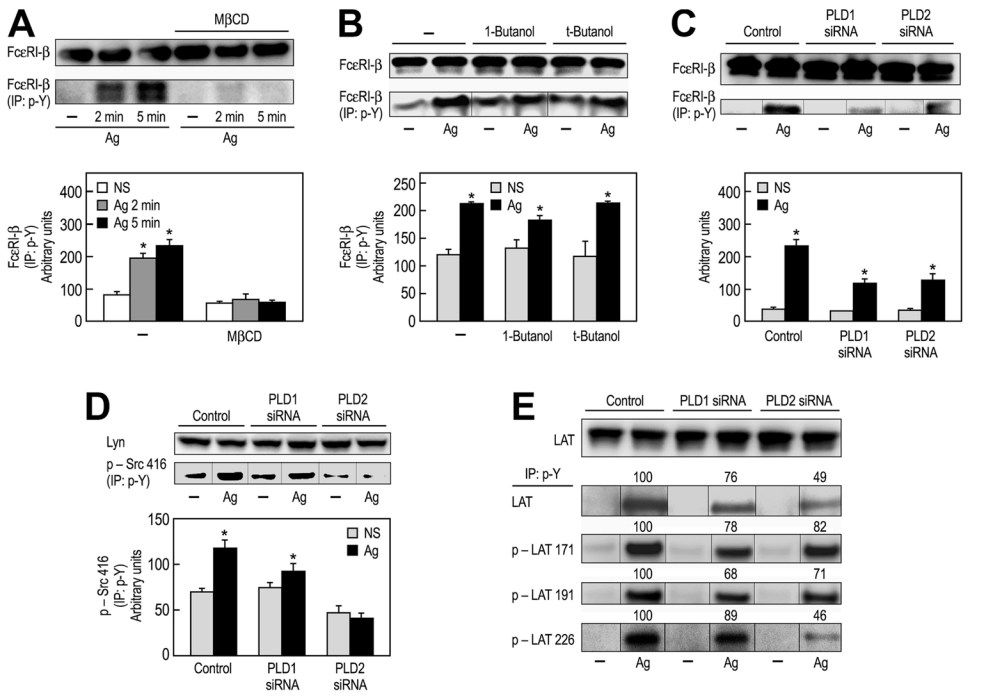

FIGURE 7.

Effects of methyl *β*-cyclodextrin, 1-butanol, and knockdown of the PLDs on early phosphorylation events in RBL-2H3 cells. Cells were treated with methyl *β*-cyclodextrin (M*β*CD) for 30 min (*A*), butanol (*B*) for 15 min, or transfected with siRNAs against the PLDs (*C–E*). Cells were stimulated or not with Ag (Ag, 100 ng/ml DNP-BSA) to achieve optimal phosphorylation of the proteins examined (2 to 5 min). Immunoblots were prepared from whole cell lysates (upper blots in each panel) or after immunoprecipitation (IP) with anti-phosphotyrosine (p-Y) Ab (lower immunoblots). Immunoblots were probed with Abs against the indicated protein. Note that Ab against phospho-Src 416 cross reacts with the equivalent phosphorylation site in Lyn. The bar graphs in *A*, *B*, *C*, and *D*, and numeric data in *E* depict densitometric data for immunoblots prepared from immunoprecipitates. Values are mean ± SEM from three experiments.